Desalination and Water Treatment
www.deswater.com

doi: 10.1080/19443994.2016.1189700

57 (2016) 26765–26772
November

Taylor & Francis
Taylor & Francis Group

Photodegradation and permeability of conventional photocatalytic reactor and two different submerged membrane photocatalytic reactors for the removal of humic acid in water

Jong-Tae Jung[a], Won-Hee Lee[b], Jong-Oh Kim[b,*]

[a]*Hansu Co., Ltd., Sandan-ro, 35Beon-ji, Danwon-gu, Ansan-si, Gyeonggi-do 425-851, Korea*
[b]*Department of Civil and Environmental Engineering, Hanyang University, 222 Wangsimni-ro, Seongdong-gu, Seoul 133-791, Korea, Tel. +82 2 2220 0325; Fax: +82 2 2220 1945; email: jk120@hanyang.ac.kr (J.-O. Kim)*

Received 4 December 2015; Accepted 24 December 2015

ABSTRACT

The combination of photocatalytic reactor with membrane provided considerable advantages over the conventional photocatalytic reactor. In this study, photodegradation and permeability of photocatalytic reactor system with and without membrane were assessed for the removal of HA. TiO_2 particles were completely rejected membranes with nominal pore size of <0.4 μm. Membranes used in submerged photocatalytic membrane reactor (SMPR) were hollow fiber MF membrane and anodizing TiO_2 membrane. The results show that photocatalytic reactor with hollow fiber MF membrane was more efficient photodegradation than that without membrane due to the synergistic effect by integration of photocatalytic reaction and membrane filtration, whereas SMPR with anodizing TiO_2 membrane showed lower treatment efficiency compared to that conventional photocatalytic reactor and SMPR with hollow fiber membrane owing to the reduction of photocatalytic activity sites. Moreover, it was revealed that permeation decrease rate of membrane with UV light irradiation was lower than that without UV light irradiation due to the reduction of membrane fouling by photocatalytic degradation of HA. Therefore, this work seems promising way to enhance photodegradation and to improve defect of conventional photocatalytic reactor.

Keywords: Humic acid; Photodegradation; Hollow fiber membrane; Photocatalytic reactor; TiO_2 membrane

1. Introduction

Natural organic matter (NOM), which mainly composed humic substances such as fulvic and humic acid (FA and HA), is one of the main sources of pollution in surface water and is a primary target of water treatment processes [1,2]. Negative effects of humic substances include undesirable color and taste, absorption and concentration of organic pollutants, and biochemical decomposition in the water distribution systems [3]. They have trihalomethanes formation potential, being precursors of trihalomethanes formed during chlorination [4]. Photocatalytic degradation technique using TiO_2 is becoming increasingly popular for the

---

*Corresponding author.

Presented at the 8th International Desalination Workshop (IDW) 2015, November 18–21, 2015, Jeju Island, Korea

removal of toxic and refractory organic compounds owing to its photoactivity, inexpensive price, stability and availability [5,6]. Nevertheless, photocatalysis is still limited to water treatment application. Systems with supported catalyst have been preferred because of operational convenience in terms of catalyst conservation and effluent-water/catalyst separation. However, such systems own one intrinsic defect, which is low efficiency due to poor mass transfer [7]. On the contrary, suspended photocatalytic reactors, which have remarkably higher mass transfer rate, have been held back exactly by the problems of catalyst conservation and water/catalyst separation [8]. In fact, it was reported that TiO_2 particles, while suspended, had removal efficiency better than the immobilized ones [9,10]. The integration of photocatalysis process with microfiltration (MF) and ultrafiltration (UF) has been intensively studied due to the perceived potential benefits that might be possible through the combination of these processes. MF not only aids in the separation of suspended catalysts but also improves the effluent quality by selective separation at molecular level. In addition, photocatalysis is able to mineralize compounds causing membrane fouling, resultingly enhancing the membrane's operation [11,12]. The synergistic effects of photocatalysis and membrane separation were reported by numerous researchers [13–15].

In this study, photodegradation and permeability of photocatalytic reactor system with and without membrane were examined for the removal of HA. The optimum conditions of operating parameters, which were TiO_2 loading and initial HA concentration, were also assessed in terms of COD_{Cr} and color.

2. Material and methods

2.1. HA solution

HA was supplied by Sigma Aldrich and had a molecular weight of 4,000–23,000 Da. HA stock solution was prepared by mixing 1 g of HA in 1 L of 0.1 N sodium hydroxide over 4 h. Stirred stock solution was filtered through a Whatman No. 1 filter paper to remove insoluble particles and stored in refrigerator at 4˚C. Degradation efficiency of HA concentration was investigated at 20, 30, and 40 mg/L of HA. All HA solutions were prepared by deionized water produced from a Barnstead Nanopure II water purification with a resistivity of 18.2 MΩcm.

2.2. Membranes

Two different membranes used in this study were hollow fiber MF membrane made of polyvinylidene fluoride (PVDF) and TiO_2 metal membrane. Hollow fiber MF membrane with a nominal pore size of 0.4 μm was provided by Energy & Environmental Co., Ltd, Korea, which was an effective filtration area of 0.11 m^2, a diameter of 30 mm and a length of 230 mm. Microporous tubular titanium metal membrane with a nominal pore size of 0.5 μm was supplied by Fibertech, Co., Ltd, Korea, which was 12 mm of inner diameter and 150 mm of length, was prepared for the anode material. Prior to anodization, titanium metal membrane was ultrasonically cleaned in deionized water, methanol, and acetone. For membrane fabrication, we used an electrolyte composition of 1 M KH_2PO_4, 0.15 M NH_4F, and 0.2 M citric acid solution. Anodization was performed at 10˚C with titanium as anode and silver as counterpart electrode. For phase transition to anatase phase of self-organized TiO_2 nanotube, heat treatment was conducted to 30-min heating at 550˚C after anodization. Stainless steel (SUS 316L) metal membrane with a nominal pore size of 0.2 μm was supplied by Hitachi, Co., Ltd, Japan, which was an effective filtration area of 0.01 m^2, 50 mm of diameter and 100 mm of length.

2.3. Experimental setup and operation

Fig. 1 shows the diagram of submerged membrane photocatalytic reactor experimental setup, which is composed of a photocatalytic reactor and hollow fiber MF membrane module. The reactor was a cylindrical tank with a working volume of 3.1 L and membrane module was placed in its center. TiO_2 powder using commercial Degussa P-25 (Degussa-Enonic, Germany) with a BET surface area of 50 m^2/g, average primary

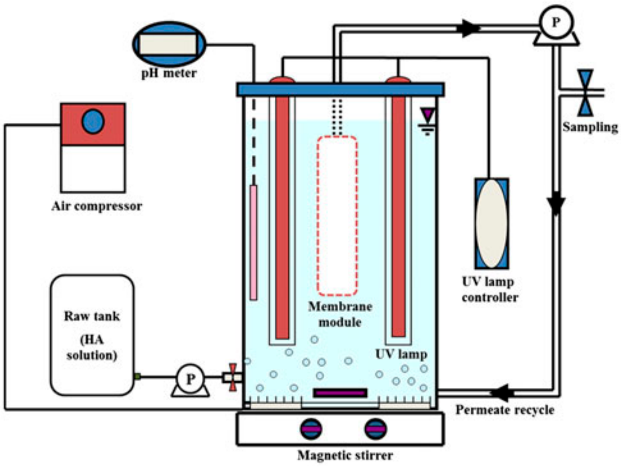

Fig. 1. A schematic of the submerged membrane photocatalytic reactor.

Table 1
Clean condition of membrane in SMPR

Method	Time (min)	Concentration	Cleaning
Air backwashing	3	20 L/min	Physical
Distilled water	5	Suction pressure × 2 times	Physical
NaOH	5	0.1 N	Chemical
Distilled water	5	Suction pressure	Physical
HCl	5	0.1 N	Chemical
Distilled water	5	Suction pressure	Physical
Sonication	5	–	Physical

particle size of 21 nm and density of 3.7 g/cm^3, was suspended in the reactor with a normal concentration of 0.1–0.6 g/L. And then pH of TiO_2 suspension was 7 ± 0.2, adjusting by 0.1 N NaOH and 0.1 N HCl. UV-C irradiation was provided by four 8 W low-pressure mercury vapor lamps located on the four sides of photocatalytic reactor. The lamps had a maximum light intensity output at 254 nm. During the operation, temperature was kept constant at 20 ± 1℃ by recirculating cooling water. Air sparging was used to supply oxygen into the reactor and to reduce the adsorption of TiO_2 particles on the membrane surface at the rate of 5 L/min. In conventional photocatalytic reactor test, several parameters were examined including TiO_2 doses from 0.1 to 0.6 g/L and initial HA concentration from 20 to 40 mg/L in order to optimize the operating conditions of the photoreactor. HA degradation efficiency of parameters was evaluated in terms of COD_{Cr} and color. The optimal conditions of TiO_2 loading and initial HA concentration determined at conventional photocatalytic reactor test were used to investigate the performance of submerged membrane photocatalytic reactor (SMPR). SMPR, using identical conditions in common with conventional photocatalytic reactor test, was assessed at pH 7 ± 0.2, UV intensity 64 W and temperature 20 ± 1℃ and was operated at 23 kPa of suction pressure. Membrane permeate was returned to the reactor to maintain the reactor volume at a constant level, excepting the minimal amount of samples taken. At the end of each experiment, membrane surface turned to be brown due to the deposition of HA. Therefore, membranes were rinsed by cleaning procedures, and a clean water test was performed to check the membrane permeability. Membrane cleaning procedure was indicated in Table 1.

2.4. Analysis

Samples were collected from each sampling port of system at regular time intervals. TiO_2 suspension samples of conventional photocatalytic reactor experiment were filtered through pre-treatment step (0.45 μm Millipore syringe filters), whereas SMPR permeates were measured without any filtration step owing to not contain any TiO_2 particle. HA degradation efficiency, expressed in terms of COD_{Cr} and color, was measured with the model HS 3100 (Humas, Korea) and DR 2010 (Hach, USA). TiO_2 separation was examined with DR 2010 (HACH, USA) by observing turbidity. A pH was measured using a MP 120 pH meter. Morphologies of TiO_2 membrane were observed using an energy-dispersive X-ray spectroscopy (EDS) and a field emission scanning electron microscope (SEM, Philips XL30 ESEM-FEG).

3. Results and discussion

3.1. TiO_2 particles separation of membranes

Three different membranes, which were hollow fiber MF membrane of nominal pore size 0.4 μm, tubular titanium membrane of nominal pore size 0.5 μm and plate-type metal membrane of nominal pore size 0.2 μm, were used to investigate the separation of TiO_2 particle in TiO_2 suspension. Experiments were conducted in conditions of suction pressure 23 kPa,

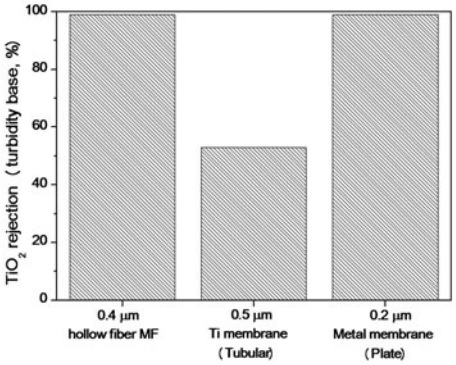

Fig. 2. TiO_2 particles separation on three different membranes (conditions: reaction time 100 min, pH 7, temperature 20 ± 1℃, TiO_2 0.3 g/L, air flow rate 5 L/min).

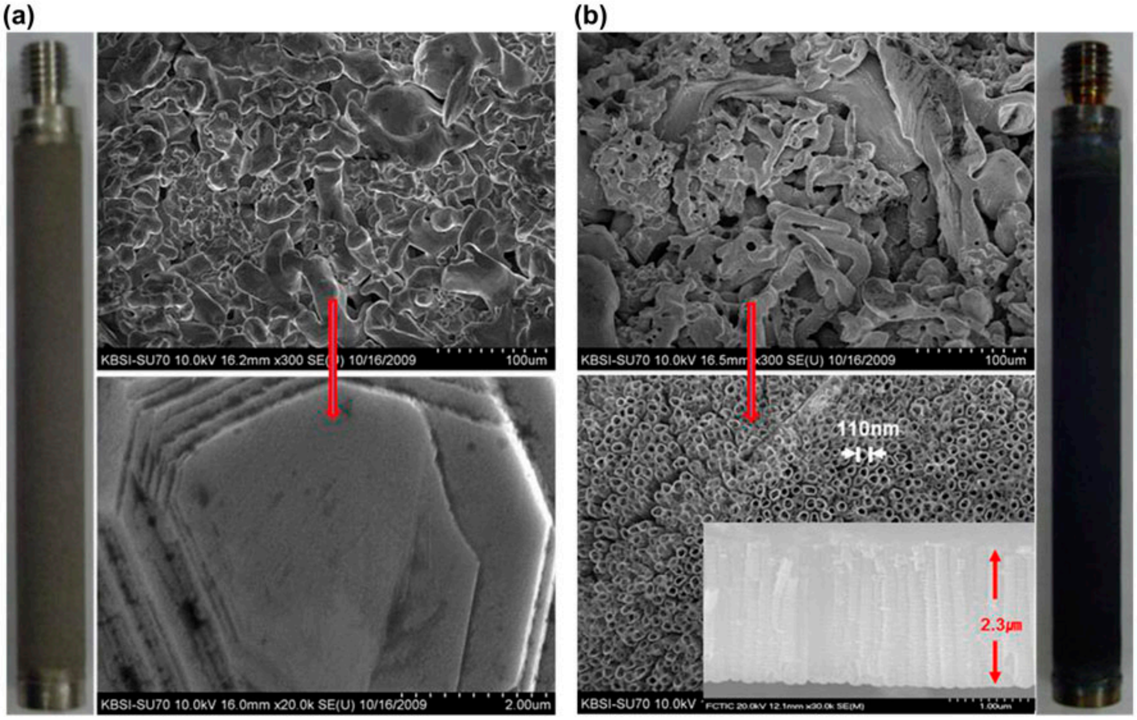

Fig. 3. SEM images of (a) titanium membrane and (b) anodized titanium dioxide membrane.

pH 7 ± 0.2, TiO_2 0.3 g/L, and operating time 100 min, and were examined in terms of turbidity. Fig. 2 shows the separation performance of TiO_2 particles for three different membranes. It can be seen that after filtration time 100 min, the complete separation of TiO_2 particles from suspension was possible by rejecting hollow fiber MF membrane and plate-type metal membrane with nominal pore size 0.4 and 0.2 μm, respectively. However, titanium membrane with pore size 0.5 μm was not effective for the separation of TiO_2 particles by showing less than 60% of turbidity in permeate. Because, the zeta potential of TiO_2 is generally strong, causing the TiO_2 particle and the Ti membrane to be under repulsive force that will cause the permeability

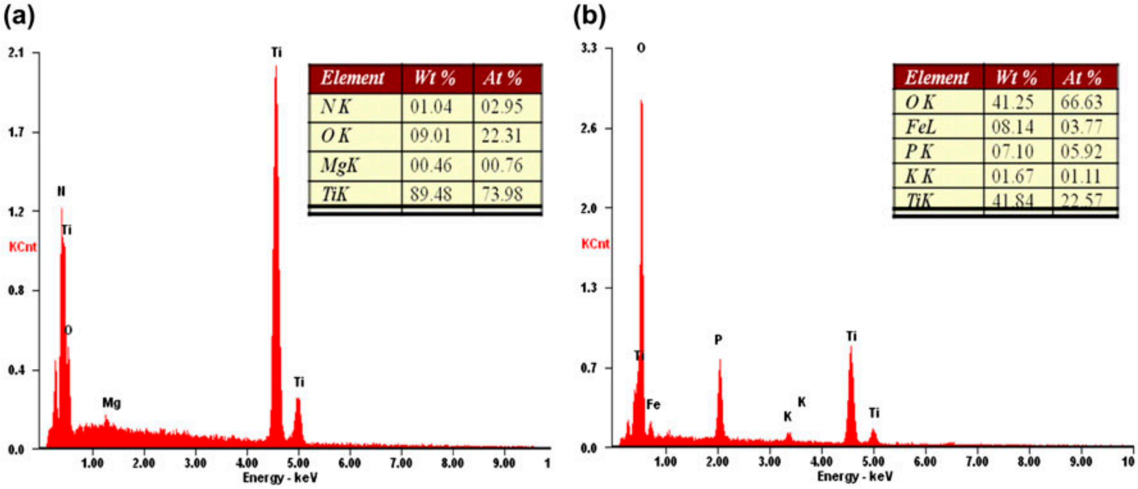

Element	*Wt %*	*At %*
N K	01.04	02.95
O K	09.01	22.31
MgK	00.46	00.76
TiK	89.48	73.98

Element	*Wt %*	*At %*
O K	41.25	66.63
FeL	08.14	03.77
P K	07.10	05.92
K K	01.67	01.11
TiK	41.84	22.57

Fig. 4. Energy-dispersive X-ray spectroscopy (EDS) of (a) titanium membrane and (b) titanium dioxide membrane fabricated by 30-min heating at 550°C after anodization.

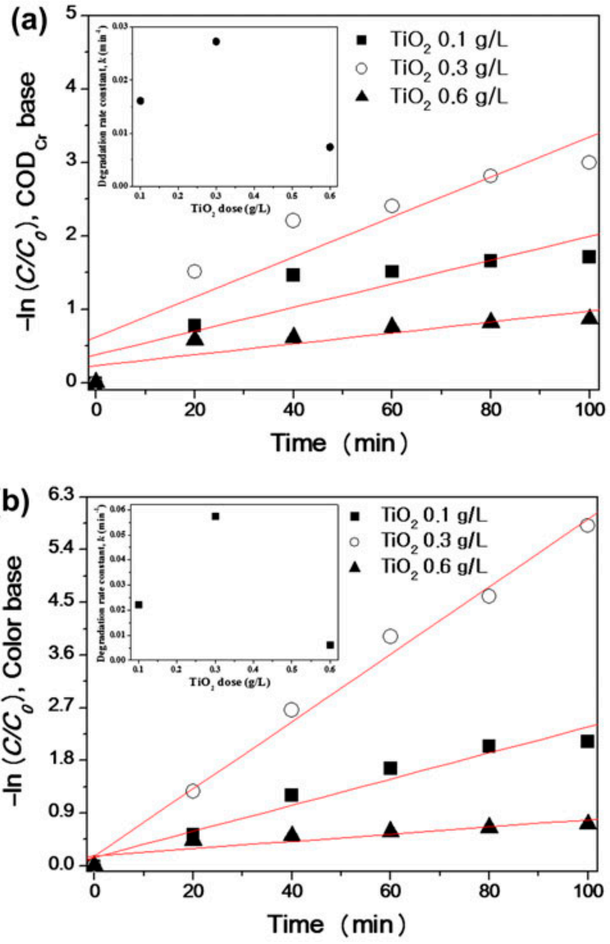

Fig. 5. Effect of photocatalyst loading with different concentrations of TiO_2 (a) COD_{cr} and (b) Color base degradation (conditions: reaction time 100 min, pH 7, temperature 20 ± 1˚C, UV intensity 64 W, HA 20 mg/L, air flow rate 5 L/min).

efficiency to drop. This titanium membrane was used to fabricate photocatalytic membrane and then was formed into TiO_2 photocatalytic membrane by anodization. In SMPR tests, we applied hollow fiber MF membrane with nominal pore size of 0.4 μm and the anodized TiO_2 membrane.

3.2. Morphology and structure of TiO_2 membrane

Fig. 3 shows the SEM images of untreated titanium membrane and TiO_2 membrane fabricated by anodization at 21 V for 1 h. Titanium membrane was anodized to make a tubular membrane with TiO_2 nanotube arrays. A large amount of TiO_2 nanotube arrays were easily obtained by anodization (as shown in Fig. 3(b)). It can be seen that TiO_2 nanotube arrays have an average of diameter of about 75 nm and length of about 2.3 μm. In order to analyze chemical composition of titanium membrane and TiO_2 membrane, EDS was indicated in Fig. 4. The EDS of titanium membrane was composed of elements, 73.98 At% Ti and 22.31 At% O, whereas EDS of TiO_2 membrane by 30-min heating at 550˚C after anodization was composed of elements, 22.57 At% Ti and 66.63 At% O. It reveals that EDS result successfully verified the formation of TiO_2 nanotube arrays by anodization owing to the increase of oxygen atomic ratio in comparison with titanium membrane.

3.3. Optimum conditions of operating parameters in conventional photocatalytic reactor tests

The amount of TiO_2 loading is one of the main parameters in a suspension photocatalytic reactor

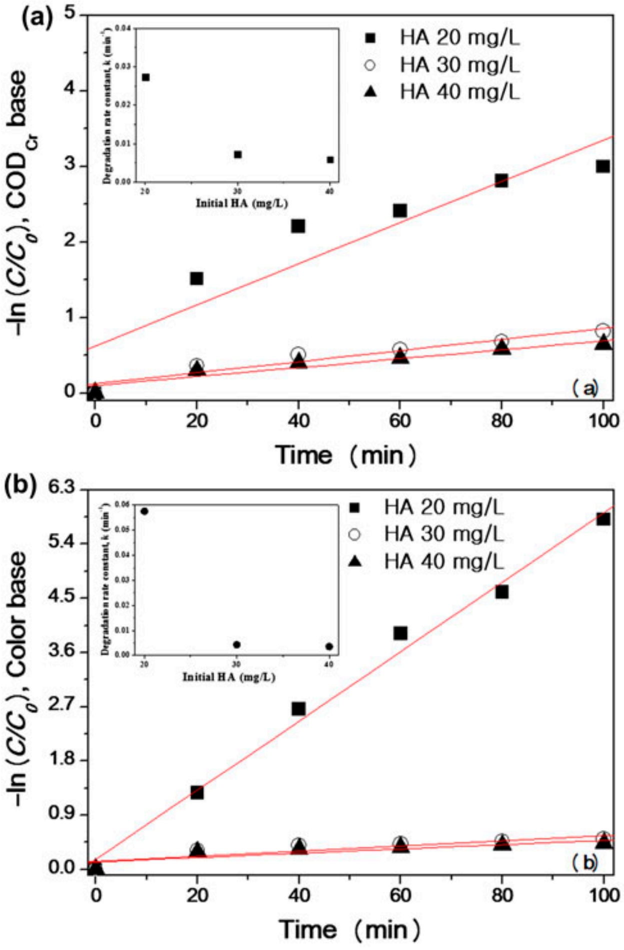

Fig. 6. Effect of initial HA concentration on normalized HA concentration (a) COD_{cr} and (b) color base degradation (conditions: reaction time 100 min, pH 7, temperature 20 ± 1˚C, UV intensity 64 W, TiO_2 0.3 g/L, air flow rate 5 L/min).

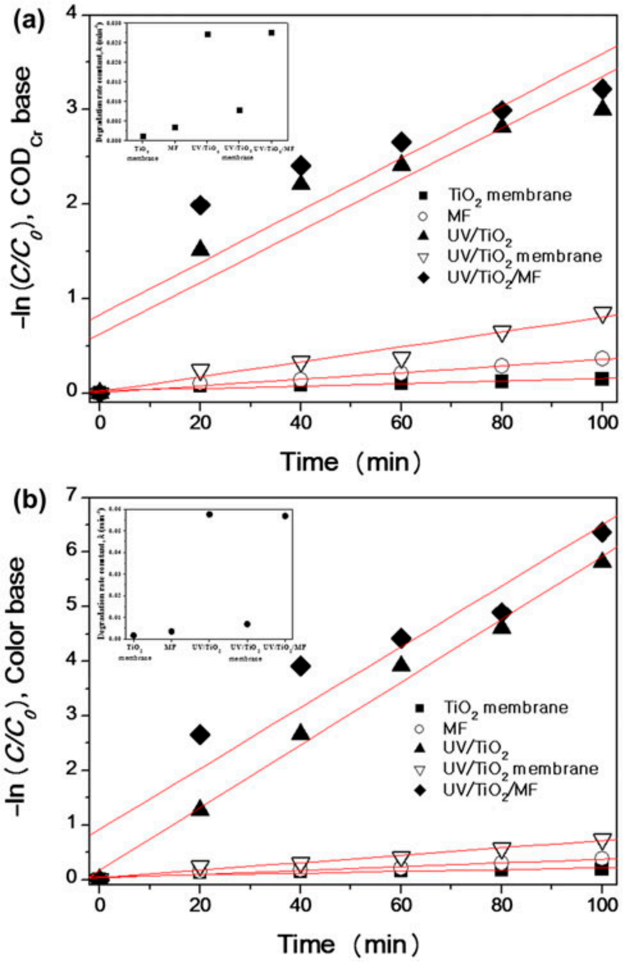

Fig. 7. Comparison of treatment efficiency on the degradation of HA at five different processes (a) COD_{cr} and (b) color base degradation (conditions: reaction time 100 min, pH 7, temperature 20 ± 1°C, UV intensity 64 W, TiO_2 0.3 g/L, HA 20 mg/L, air flow rate 5 L/min).

system. Generally, when the catalyst loading is increased, there is an increase in the surface area of the catalyst available for adsorption and degradation. On the other hand, an increase in the photocatalyst concentration increases the solution opacity leading to a decrease in the penetration of photo flux in the reactor [16]. Consequently, we examined the effect of TiO_2 loading. The results investigated were shown in Fig. 5. In this study, it was found that the removal of COD_{Cr} and color increases with increasing TiO_2 loading, especially up to TiO_2 concentration of 0.3 g/L. The 0.6 g/L of TiO_2 concentration resulted in the lowest degradation. This may be ascribed to the agglomeration of TiO_2 particles and to the decrease of UV light penetration by increasing the opacity of the suspension. Thus, the optimum TiO_2 concentration for the removal of COD_{Cr} and color was 0.3 g/L. Similar study results of TiO_2 loading effect on the photocatalytic activity were also reported by [17,18]. The effect of initial HA concentration on the photocatalytic oxidation of HA was investigated by varying the initial HA concentration from 20 to 40 mg/L with an optimum TiO_2 concentration of 0.3 g/L, and results were indicated in Fig. 6. It can be seen that the photodegradation of HA is considerably influenced by the initial concentration of HA, thus COD_{Cr} and color degradation of HA decrease with increasing initial concentration. It is likely that the path length of photons entering TiO_2 at higher HA concentration decreases due to the UV-screening effect (as inner filter action) of HA itself. Therefore, the optimum initial concentration of HA was 20 mg/L. Similarly [19] reported that reaction rate decreased with the increase in initial concentration of HA.

3.4. Comparison of conventional photocatalytic reactor and submerged membrane photocatalytic reactors on the degradation of HA

In order to assess the treatment efficiency of photocatalytic reactor with/without submerged membrane on the degradation of HA, experiments were conducted in conditions of suction pressure 23 kPa, UV intensity 64 W, pH 7 ± 0.2 as well as the optimum conditions of TiO_2 0.3 g/L and initial HA concentration 20 mg/L determined in conventional photocatalytic reactor and then were operated to evaluate the relative removal efficiency of MF, TiO_2 membrane, UV/TiO_2, UV/TiO_2/MF, and UV/TiO_2 membrane. Degradation efficiencies were calculated from COD_{Cr} and color. The results were displayed in Fig. 7. The degradation efficiency of COD_{Cr} and color for the MF alone without UV irradiation was about 31 and 32%, whereas COD_{Cr} and color of TiO_2 membrane alone were approximately 14 and 17%, respectively. The removal efficiency of MF alone was relatively higher than that of TiO_2 membrane alone. It is likely that HA molecules can be easily separated by MF having a smaller nominal pore size. In contrast, degradation efficiency of HA was highly enhanced by UV irradiation with TiO_2 and TiO_2 membrane. However, TiO_2 membrane coupled photocatalytic reactor was showed lower treatment efficiency than conventional photocatalytic reactor with the suspension of TiO_2 particles. This is because BET surface area of TiO_2 powder was higher 10 times than that of TiO_2 membrane. On the other hand, application of submerged MF with photocatalytic reactor exhibited the faster and better degradation performance than photocatalytic reactor without the presence of membrane due to the synergistic effect by integration. The synergistic effect might result from the enhanced mass transfer in photocatalytic reaction by membrane filtration. Consequentially, it showed that submerged membrane photocatalytic reactor system is very effective treatment process for the degradation of HA, especially composing of TiO_2 powder rather than immobilized TiO_2.

3.5. Submerged membrane filtration performance

In order to assess the permeability of two different membranes in photocatalytic reactor, experiments were conducted for 100 min at suction pressure of 23 kPa and initial HA concentration of 20 mg/L. TiO_2 loading of 0.3 g/L was added in hollow fiber MF photocatalytic reactor test. Nominalized flux and permeation decrease rate of membranes with and without UV irradiation were shown in Fig. 8. It can be seen that a sharp flux decline was observed in TiO_2 membrane photocatalytic reactor without UV irradiation and after 100-min permeation decrease rate was about 70%. This was due to deposition of HA on the membrane surface, thus leading to membrane fouling. However, permeation decrease rate of TiO_2 membrane with UV irradiation was about 21%, which was enhanced over 60% compared to that of TiO_2 membrane without UV irradiation. In hollow fiber membrane photocatalytic reactor test, permeation decrease rate of hollow fiber membrane without UV light irradiation was approximately 25% after 100 min of filtration time, whereas there was no change in permeation decrease rate of hollow fiber membrane with UV light irradiation. It can be explained that the effective photocatalytic degradation of HA prevented membrane from fouling obviously.

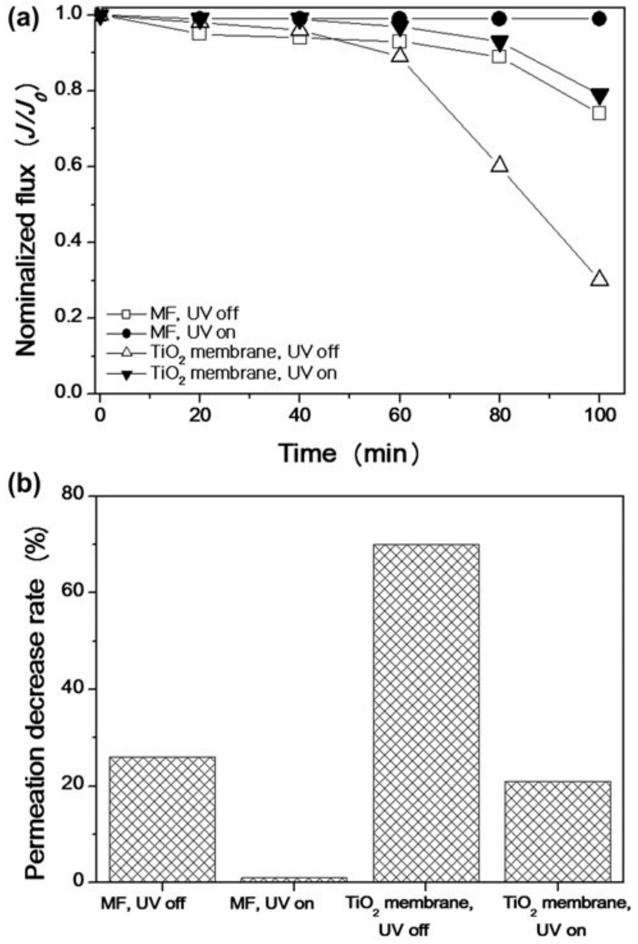

Fig. 8. Permeability of membranes with and without UV light irradiation (a) nominalized flux and (b) permeation decrease rate (conditions: reaction time 100 min, pH 7, temperature 20 ± 1°C, UV intensity 64 W, TiO_2 0.3 g/L, HA 20 mg/L, air flow rate 5 L/min).

4. Conclusions

This study investigated photodegradation and permeability of photocatalytic reactor with and without membrane for the removal of HA. Several conclusions made from this study are as follows:

TiO_2 particles were completely rejected by hollow fiber membrane with nominal pore size of 0.4- and 0.2-μm plate-type metal membrane whereas 0.5-μm titanium membrane was not effectively separate.

Immobilized TiO_2 nanotube membrane was fabricated by anodization and was confirmed through the analysis of SEM and EDX.

The optimum conditions of TiO_2 loading and initial HA concentration in photocatalytic reactor system for the removal of HA were 0.3 and 20 mg/L, respectively.

The highest degradation performance of HA was observed in photocatalytic reactor with hollow fiber membrane owing to the synergistic effect by integration of photocatalytic reaction and membrane filtration.

Permeation decrease rate of membrane with UV light irradiation was lower than that without UV light irradiation due to the reduction of membrane fouling by photocatalytic degradation of HA.

Acknowledgment

This study was supported by a National Research Foundation of Korea (NRF) grant funded by the Korean Government (NRF-2013R1A2A1A09007252).

References

[1] J. Chen, B. Gu, E.J. LeBoeuf, H. Pan, S. Dai, Spectroscopic characterization of the structural and functional properties of natural organic matter fractions, Chemosphere 48 (2002) 59–68.

[2] T. Zhou, T.-T. Lim, S.-S. Chin, A. Fane, Treatment of organics in reverse osmosis concentrate from a municipal wastewater reclamation plant: Feasibility test of advanced oxidation processes with/without pretreatment, Chem. Eng. J. 166 (2011) 932–939.

[3] M. Aeschbacher, S.H. Brunner, R.P. Schwarzenbach, M. Sander, Assessing the effect of humic acid redox state on organic pollutant sorption by combined electrochemical reduction and sorption experiments, Environ. Sci. Technol. 46 (2012) 3882–3890.

[4] S.-K. Kam, J. Gregory, The interaction of humic substances with cationic polyelectrolytes, Water Res. 35 (2001) 3557–3566.

[5] Z. Ai, P. Yang, X. Lu, Degradation of 4-chlorophenol by a microwave assisted photocatalysis method, J. Hazard. Mater. 124 (2005) 147–152.

[6] V. Reguero, R. López-Fernández, J. Fermoso, O. Prieto, P. Pocostales, R. González, R. Irusta, S. Villaverde, Comparison of conventional technologies and a Submerged Membrane Photocatalytic Reactor (SMPR) for removing trihalomethanes (THM) precursors in drinking water treatment plants, Desalination 330 (2013) 28–34.

[7] R.L. Pozzo, M.A. Baltanás, A.E. Cassano, Towards a precise assessment of the performance of supported photocatalysts for water detoxification processes, Catal. Today 54 (1999) 143–157.

[8] X. Huang, Y. Meng, P. Liang, Y. Qian, Operational conditions of a membrane filtration reactor coupled with photocatalytic oxidation, Sep. Purif. Technol. 55 (2007) 165–172.

[9] R.-Y. Horng, C. Huang, M.-C. Chang, H. Shao, B.-L. Shiau, Y.-J. Hu, Application of TiO_2 photocatalytic oxidation and non-woven membrane filtration hybrid system for degradation of 4-chlorophenol, Desalination 245 (2009) 169–182.

[10] D. Robert, A. Gauthier, Prospects for a supported photocatalyst in the detoxification of drinking water, Water Qual. Int. (1998) 27–28.

[11] D. Ho, S. Vigneswaran, H.H. Ngo, Photocatalysis-membrane hybrid system for organic removal from biologically treated sewage effluent, Sep. Purif. Technol. 68 (2009) 145–152.

[12] S. Mozia, A.W. Morawski, Hybridization of photocatalysis and membrane distillation for purification of wastewater, Catal. Today 118 (2006) 181–188.

[13] V. Kochkodan, E. Rolya, V. Goncharuk, Photocatalytic membrane reactors for water treatment from organic pollutants, J. Water Chem. Technol. 31 (2009) 227–237.

[14] V. Loddo, V. Augugliaro, L. Palmisano, Photocatalytic membrane reactors: Case studies and perspectives, Asia-Pac. J. Chem. Eng. 4 (2009) 380–384.

[15] G. Zhang, L. Yao, L. Wang, J. Zhang, L. Xu, Z. Fan, Photocatalytic membrane reactor used for water and wastewater treatment, Recent Pat. Eng. 6 (2012) 127–136.

[16] S. Mozia, Photocatalytic membrane reactors (PMRs) in water and wastewater treatment. A review, Sep. Purif. Technol. 73 (2010) 71–91.

[17] S.S. Chin, T.M. Lim, K. Chiang, A.G. Fane, Factors affecting the performance of a low-pressure submerged membrane photocatalytic reactor, Chem. Eng. J. 130 (2007) 53–63.

[18] V. Sarasidis, S. Patsios, A. Karabelas, A hybrid photocatalysis–ultrafiltration continuous process: The case of polysaccharide degradation, Sep. Purif. Technol. 80 (2011) 73–80.

[19] X. Li, C. Fan, Y. Sun, Enhancement of photocatalytic oxidation of humic acid in TiO_2 suspensions by increasing cation strength, Chemosphere 48 (2002) 453–460.